Original article

UDC 542.06

DOI: 10.57070/2304-4497-2025-3(53)-51-62

EVALUATION OF TITANIUM DIOXIDE NANOTUBE STRUCTURE BY ULTRASONIC-HYDROTHERMAL SYNTHESIS METHOD FOR CORROSION INHIBITOR STORAGE APPLICATION

© 2025 V. Z. Vu, H. B. Nguyen, R. I. Nigmetzyanov

Moscow Automobile and Road Construction State Technical University (MADI) (64 Leningradsky Prospekt, Moscow, 125319, Russian Federation)

Abstract. This study presents the synthesis of TiO_2 nanotubes using a combined hydrothermal–ultrasonic approach with short hydrothermal durations ranging from 4 to 10 hours, aiming to evaluate the controllability of morphology and crystalline structure for anticorrosion applications. Ultrasonic pretreatment was applied to enhance precursor dispersion and promote the formation of ordered nanotubular structures, thereby reducing synthesis time compared with conventional hydrothermal processes. The obtained materials were characterized using several complementary techniques: scanning electron microscopy (SEM) to analyze morphology and nanotube distribution, Raman spectroscopy and X-ray diffraction (XRD) to assess phase composition and crystallinity, and Fourier-transform infrared spectroscopy (FTIR) to identify surface bonding features. The results revealed apparent differences in nanotube organization, crystallinity, and phase development depending on the reaction duration, confirming that synthesis time plays a decisive role in tailoring structural parameters. These findings demonstrate that the hydrothermal–ultrasonic method provides an efficient and versatile route for fabricating TiO_2 nanotubes with tunable structural and functional properties. Furthermore, the synthesized nanostructures exhibit strong potential as carriers of corrosion inhibitors, enabling improved storage and controlled release within polymer-based protective coatings, thereby contributing to the development of next-generation anticorrosion technologies.

Keywords: TiO_2 nanotubes, ultrasonic-hydrothermal method, reaction time, corrosion inhibitor storage capacity

Acknowledgments. The material was prepared as part of scientific research under project No. FSFM-2024-0001

For citation: Vu V.Z., Nguyen H.B., Nigmetzyanov R.I. Evaluation of titanium dioxide nanotube structure by ultrasonic-hydrothermal synthesis method for corrosion inhibitor storage application. *Bulletin of the Siberian State Industrial University*. 2025;3(53):51–62. *http://doi.org/10.57070/2304-4497-2025-3(53)-51-62*

ОЦЕНКА СТРУКТУРЫ НАНОТРУБОК ДИОКСИДА ТИТАНА, СИНТЕЗИРОВАННЫХ УЛЬТРАЗВУКОВО-ГИДРОТЕРМАЛЬНЫМ МЕТОДОМ, ДЛЯ ПРИМЕНЕНИЯ В ХРАНЕНИИ ИНГИБИТОРОВ КОРРОЗИИ

© 2025 г. В. З. Ву, Х. Б. Нгуен, Р. И. Нигметзянов

Московский автомобильно-дорожный государственный технический университет (Россия 125319, Москва, Ленинградский проспект, 64)

Аннотация. В настоящем исследовании представлен синтез нанотрубок TiO_2 с использованием комбинированного гидротермального и ультразвукового подходов с короткими выдержками от 4 до 10 ч для оценки управляемости морфологии и кристаллической структуры для антикоррозионных приложений. Ультразвуковая предподготовка улучшала диспергирование прекурсора и способствовала формированию упорядоченных нанотрубчатых структур, сокращая время синтеза по сравнению с традиционными методами. Полученные материалы были исследованы с помощью сканирующей электронной микроскопии (СЭМ) для анализа морфологии и распределения нанотрубок, спектроскопии Рамана и рентгеноструктурного анализа (РСА) для оценки фазового состава и кристалличности, а также

инфракрасной спектроскопии с преобразованием Фурье (ИК-Фурье) для изучения поверхностных связей. Результаты показали различия в организации нанотрубок, кристалличности и фазовом развитии в зависимости от времени реакции, подтверждая ключевую роль длительности синтеза в формировании структурных параметров. Рассматриваемый гибридный метод представляет собой эффективную стратегию синтеза функциональных наноматериалов с улучшенной способностью к хранению и контролируемому высвобождению ингибиторов коррозии в полимерных покрывных системах.

Ключевые слова: нанотрубки TiO_2, ультразвуко-гидротермальный метод, время реакции, способность к хранению ингибиторов коррозии

Финансирование. Материал подготовлен в рамках научных исследований по проекту № FSFM-2024-0001.

Для цитирования: By В.З., Нгуен Х.Б., Нигметзянов Р.И. Оценка структуры нанотрубок диоксида титана, синтезированных ультразвуково-гидротермальным методом, для применения в хранении ингибиторов коррозии. *Вестник Сибирского государственного индустриального университета*. 2025;3(53):51–62. *http://doi.org/10.57070/2304-4497-2025-3(53)-51-62*

Introduction

The hydrothermal method for synthesizing TiO_2 nanotubes has been extensively studied and developed since 1998 [1]. However, a significant limitation of this approach is the typically prolonged synthesis time, which ranges from 24 to 72 hours, thereby reducing its practical applicability [2 – 4]. In this method, TiO_2 nanotubes are formed by reacting TiO_2 powder and a NaOH solution under hydrothermal conditions in an autoclave. To enhance the efficiency of the synthesis process, ultrasonic treatment is applied before the hydrothermal reaction. This technique facilitates uniform dispersion of TiO_2 powder in the solution, breaks apart particle agglomerates, promotes chemical reactions, and increases the interfacial contact area between the phases. Ultrasonic waves induce cavitation effects, forming microbubbles that collapse to generate localized high temperatures and pressures. These conditions accelerate dissolution and material restructuring, significantly reducing the synthesis time.

The synthesis process of TiO_2 nanotubes is influenced by various factors such as hydrothermal temperature and duration, ultrasonic power and time, acid washing procedure, and calcination temperature [5]. Adjusting reaction parameters (temperature, pressure, reagent concentration, ultrasonic power and duration, etc.) allows for effective control over the morphology and size of the nanotubes [6; 7], thereby enabling the targeted fabrication of materials with specific structural features.

The formation mechanism of TiO_2 nanotubes by the hydrothermal-ultrasonic method can be considered as follows [5; 8 – 10]:

$$n\mathrm{TiO_2} + 2\mathrm{NaOH} \rightarrow 2\mathrm{Na^+} + [\mathrm{Ti}_n\mathrm{O}_{2n+1}]^{2-} + \mathrm{H_2O}; \quad (1)$$

$$2\mathrm{Na^+} + [\mathrm{Ti}_n\mathrm{O}_{2n+1}]^{2-} \rightarrow [\mathrm{Na_2Ti}_n\mathrm{O}_{2n+1}]_{\text{nanomembrane}} \quad (2)$$

$$2\mathrm{Na^+} + [\mathrm{Ti}_n\mathrm{O}_{2n+1}]^{2-} + [\mathrm{Na_2Ti}_n\mathrm{O}_{2n+1}]_{\text{nanomembrane}} \rightarrow [\mathrm{Na_2Ti}_n\mathrm{O}_{2n+1}]_{\text{nanotube}}; \quad (3)$$

$$[\mathrm{Na_2Ti}_n\mathrm{O}_{2n+1}]_{\text{nanotube}} + \mathrm{H_2O} \rightarrow 2\mathrm{NaOH} + [\mathrm{H_2Ti}_n\mathrm{O}_{2n+1}] \xrightarrow{t^\circ} [\mathrm{TiO_2}]_{\text{nanotube}} \quad (4)$$

The diagram illustrating the formation of TiO_2 nanotubes is described in Fig. 1.

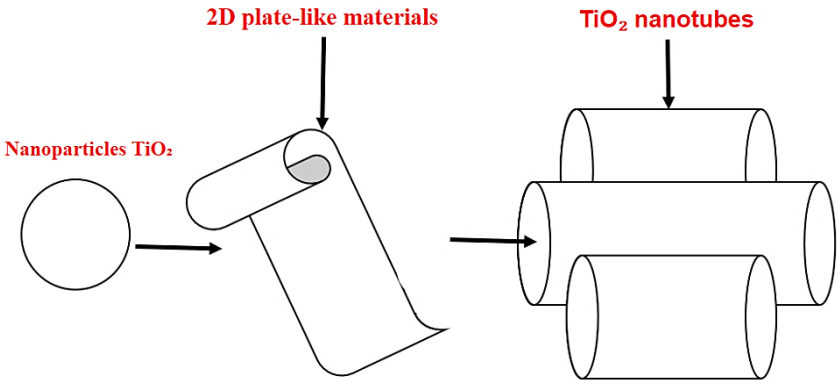

Fig. 1. Schematic illustration of the formation mechanism of TiO_2 nanotubes from TiO_2 nanoparticles
Рис. 1. Схематическая диаграмма, иллюстрирующая процесс превращения наночастиц оксида TiO_2 в нанотрубки TiO_2

Such tailored TiO_2 nanotube structures are beautiful in nanotechnology, not only for their ability to store and control the release of corrosion inhibitors, but also for their potential use as functional additives in polymer-based coatings [11 – 12]. Recent studies have shown that embedding TiO_2 nanotubes loaded with corrosion inhibitors into epoxy or other polymer matrices can significantly enhance the barrier properties and active corrosion protection of the coatings, especially in aggressive marine environments [13 – 15]. In this context, the nanotubes act as nanocontainers that provide a self-healing effect by releasing inhibitors in response to local pH changes or chloride ion attack, thereby extending the service life of metallic structures exposed to seawater.

Research Methodology

Material

Titanium dioxide "Degussa P25", sodium hydroxide, hydrochloric acid... All chemicals were used without further purification.

Research Methodology

1.5 g of TiO_2 (Degussa P25) was dispersed in 50 mL of 10 M NaOH solution and stirred for 15 minutes. The mixture was then treated with ultrasound for 2 hours at 22 Hz.

In this study, the hydrothermal procedure was designed as follows: the prepared solution was transferred into a Teflon-lined autoclave and subjected to hydrothermal treatment at 200 °C for 4, 6, 8, and 10 h, as proposed by the research group. After completion of the synthesis, the obtained product was filtered, rinsed with dilute HCl solution, and subsequently washed several times with deionized water until a neutral pH was reached.

Finally, the samples were dried and calcined at 350°C for 1 hour before being analyzed using SEM, XRD, and Raman spectroscopy.

Measurements

The material's morphology was analyzed using Scanning Electron Microscopy (SEM) on a "JEOL–4000 EX High-Resolution Electron Microscopy", X-ray crystallography (XRD) on a "Siemens D-500 X-ray Diffraction System," Raman spectroscopy using an "HRS-500 Spectrometer with a Pylon 100BR Detector", and Fourier-transform infrared spectroscopy “was performed on a Vertex 80v Fourier spectrometer in the spectral range of 400-4000 cm^{-1} with a resolution of 4 cm^{-1}”. All studies were conducted at the Institute of Solid State Physics of the Russian Academy of Sciences (Institute of Solid State Physics RAS), Russian Federation.

Results and discussion

The morphological and structural characteristics of the nanotubes synthesized by the hydrothermal-ultrasonic method were investigated using SEM analysis (Fig. 2). The analysis results reveal the typical structure of the nanotubes, with diameters ranging from 50 to 300 nm and lengths from 1 to 10 μm. SEM analysis shows that the sample synthesized hydrothermally for 4 hours exhibits a dense structure with a high tube density, while the sample synthesized hydrothermally for 6 hours shows a dense distribution of nanotubes with strong agglomeration. The samples synthesized hydrothermally for 8 and 10 hours display a more balanced structure with a more uniform distribution. The variation in nanotube density across the samples is believed to be attributed to the different conditions during the synthesis process.

According to previous studies, TiO_2 nanotubes are typically synthesized via hydrothermal treatment at 150 °C for 24 hours, resulting in nanotubes with outer diameters ranging from 3.93 to 11.44 nm and lengths between 2 and 10 μm. These structures are characterized by thin, uniform tubes with high crystallinity-suitable for applications in photocatalysis, environmental remediation, and biomedicine [9; 16; 17]. However, in this study, TiO_2 nanotubes were synthesized using a combined hydrothermal–ultrasonic method within a significantly shorter duration of 4 to 10 hours, yielding nanotubes with larger diameters ranging from 50 to 300 nm and lengths from 1 to 10 μm. Although the hydrothermal reaction time was significantly shorter than the conventional 24-hour process [16; 17], well-formed TiO_2 nanotubes with high density and comparable lengths were still successfully obtained.

The Raman spectroscopy analysis results (Fig. 3) show a significant transformation between the TiO_2 samples as a function of hydrothermal time, particularly in the phase structure changes and the characteristics of crystal lattice vibrations. The peak at 146 cm^{-1}, corresponding to the characteristic E_g mode of the anatase phase [18; 19], is visible in the samples synthesized after 4 and 6 hours, and is more potent in the hydrothermal sample for 4 hours. However, this peak almost disappears in the samples synthesized hydrothermally for 8 and 10 hours, indicating a decline in the anatase phase as the hydrothermal time is extended. Similarly, the 236 and 279 cm^{-1} peaks, associated with anatase's characteristic or second-order vibrations (such as the B_{1g} mode) [18; 19], gradually weaken and disappear in the later samples. Notably, the peak around 127 cm^{-1}, characteristic of the B_{1g} mode of the rutile phase [18; 19], only appears in the samples synthesized after 8 and 10 hours, reflecting the formation of the rutile phase under extended hydrothermal conditions. Along with this, other characteristic peaks of rutile, such as 447 cm^{-1} (E_g) and 610 cm^{-1} (A_{1g}), become increasingly prominent, further

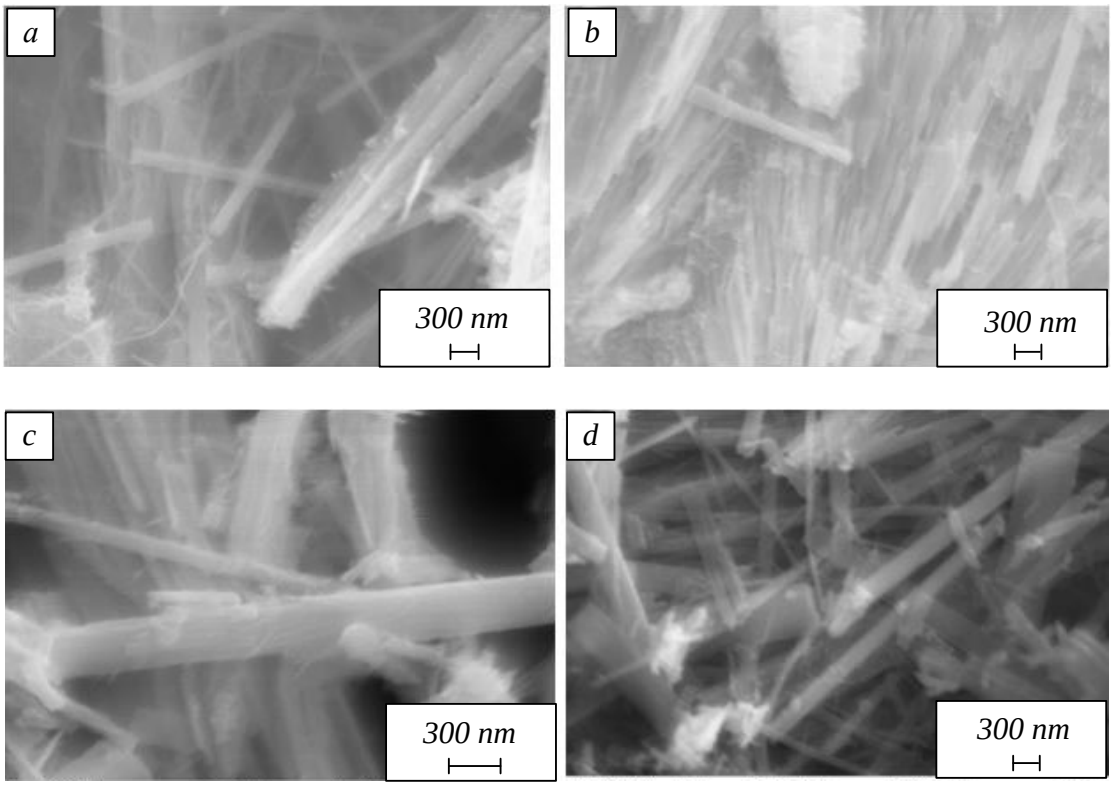

Fig. 2. SEM analysis of TiO_2 nanotube structures synthesized using a combined ultrasonic–hydrothermal treatment: *a – d* – 4; 6; 8; 10 h

Рис. 2. Структур нанотрубок TiO_2, полученных методом гидротермального синтеза при различном времени обработки: *a – d* – 4; 6; 8; 10 ч

reinforcing the observation of the phase transition from anatase to rutile [18; 19].

The evaluation of the relationship between structure and the ability to store and release corrosion inhibitors, based on SEM analysis of the synthe sized nanotube samples, shows a clear correlation between nanomorphology, crystal structure, and this ability. The hydrothermal synthesis sample at 4

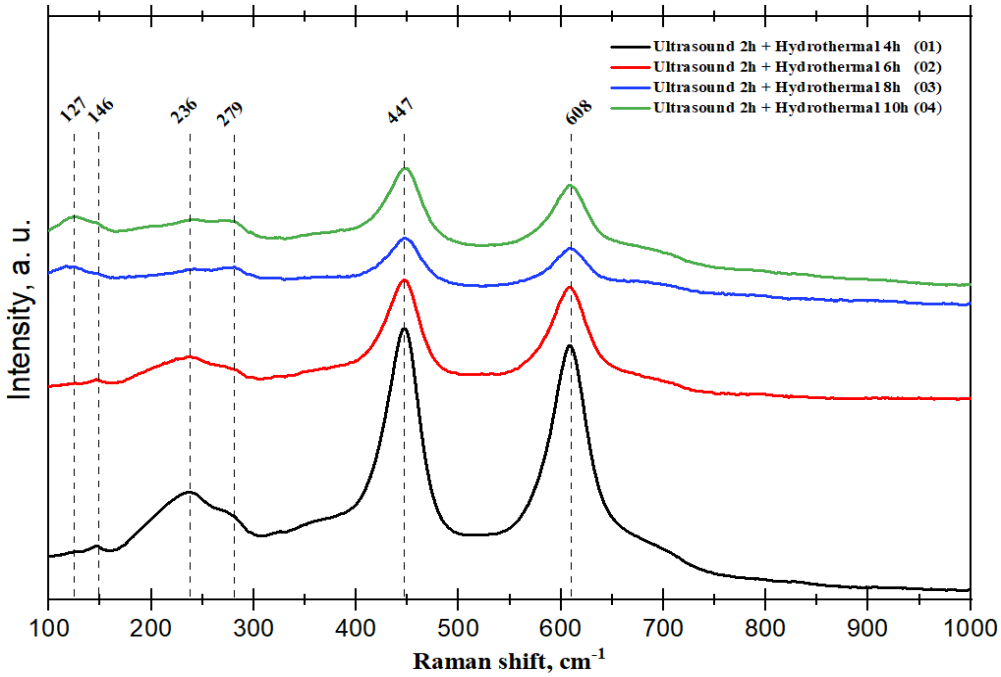

Fig. 3. Raman spectra of TiO_2 nanotube samples synthesized by combined ultrasonic-hydrothermal treatment.

Рис.3. Рамановские спектры образцов нанотрубок TiO_2, синтезированных комбинированной ультразвуково-гидротермальной обработкой

hours, with a high nanowire density (> 50 wires/μm²) and a dense structure, exhibits a prominent presence of the anatase phase, with a large surface area and a porous structure [20; 21], which facilitates the adsorption and storage of inhibitors. However, the uneven distribution and dense structure may affect the controlled release of inhibitors and reduce the dispersion efficiency within the epoxy matrix. The hydrothermal synthesis sample at 6 hours, with strong aggregation and nanoparticles on the surface, can improve adhesion to the polymer and enhance mechanical properties, but faces difficulties in the dispersion and release of inhibitors. The hydrothermal synthesis sample at 8 hours, with a dispersed tubular structure, thin tube walls, and low impurity surface, promotes the rapid diffusion of inhibitors and compatibility with epoxy. However, the low nanotube density and the clear formation of the rutile phase may reduce the corrosion inhibitor storage capacity. Finally, the hydrothermal synthesis sample at 10 hours, with a uniform structure, stable diameter, and a predominance of the rutile phase, although the adsorption capacity may be lower compared to anatase, optimized the controlled release and uniform dispersion of inhibitors in the epoxy matrix.

XRD analysis (Fig. 4) of the four TiO_2 nanotube samples reveals significant variations in crystallinity and phase composition depending on the hydrothermal reaction time. The sample synthesized for 10 hours exhibits the weakest diffraction intensity, with characteristic peaks of the layered titanate phase appearing at $2\theta \approx 10.6°$ and 20°, while rutile peaks are only faintly observed. This indicates that the material predominantly retains its original layered structure and that the phase transformation to TiO_2 remains limited. In the sample subjected to an 8-hour hydrothermal reaction, the peaks at $2\theta \approx 10.6°$ and 19.6° become more pronounced, suggesting a more evident formation of the layered titanate phase ($H_2Ti_3O_7$ or $Na_2Ti_3O_7$). At the same time, weak rutile peaks at $2\theta \approx 27.4°$ and 36.6° are still present, indicating that the material is in an intermediate stage of the phase transformation process [22; 23]. The sample reacted for 6 hours and displayed a diffraction pattern with all characteristic rutile peaks, although with lower intensities than the 4-hour sample. This suggests that crystallization is relatively complete, although a small intermediate phase may still exist. The sample synthesized for 4 hours shows the highest intensity XRD pattern, with sharp and well-defined peaks-most notably at $2\theta \approx 27.4°$, corresponding to the (110) plane of rutile TiO_2-along with other typical peaks at 36.1, 41.2, 44.0, 48.6 and 54.6° [22; 23], reflecting a high degree of crystallinity and a clear phase transformation from titanate to rutile.

A semi-quantitative estimation of the phase composition based on XRD peak intensity and sharpness was conducted for the synthesized TiO_2 nanotube samples (Table). Although a complete Rietveld refinement was not performed due to the lack of raw diffraction data, visual analysis indicates a clear trend of phase evolution with hydrothermal treatment time.

The FTIR spectra (Fig. 5) reveal the presence of characteristic absorption bands at 520, 696, 970, and 1120 cm^{-1}, clearly reflecting the structural evolution and phase composition changes of TiO_2 samples as a function of hydrothermal treatment time. The band at approximately 520 cm^{-1} is assigned to Ti – O – Ti bending vibrations characteristic of the rutile lattice. In contrast, the signal at 696 cm^{-1} corresponds to stretching vibrations of TiO_6 octahedral units, which become more pronounced when rutile predominates at shorter treatment durations. The band at 970 cm^{-1} is attributed to Ti – O stretching vibrations associated with hydroxyl groups or adsorbed water. It simultaneously indicates the development of layered titanate structures as the hydrothermal time is extended [24; 25].

The intensity of these absorption bands decreases in the following order: the 6 h sample exhibits the strongest signals, followed by the 4 h sample, whereas the 8 h and 10 h samples display a pronounced attenuation and show comparable spectral characteristics. This trend indicates that in the shorter hydrothermal treatments (4 – 6 h), the characteristic vibrations of Ti – O – Ti networks and Ti – O – hydroxyl linkages remain relatively strong, reflecting the presence of rutile and anatase phases with well-defined crystallinity. In contrast, for the longer treatment durations (8 – 10 h), the simultaneous weakening of these bands is associated with structural reorganization, in which rutile is gradually dissolved and replaced by layered titanate, resulting in nearly identical spectral features for the two samples. Such an FTIR evolution is in excellent agreement with the semi-quantitative Rietveld estimations, thereby reinforcing the evidence of a phase transition from rutile/anatase to titanate with increasing hydrothermal time.

The semi-quantitative Rietveld analysis reveals a progressive transformation in the phase composition of the nanotube samples with increasing hydrothermal duration, evolving from a rutile-dominated structure at 4 hours to a titanate-rich structure at 10 hours. This transition can be attributed to an alkali-driven dissolution-recrystallization mechanism, in which the initially stable and highly crystalline rutile phase undergoes gradual surface dissolution under concentrated NaOH conditions.

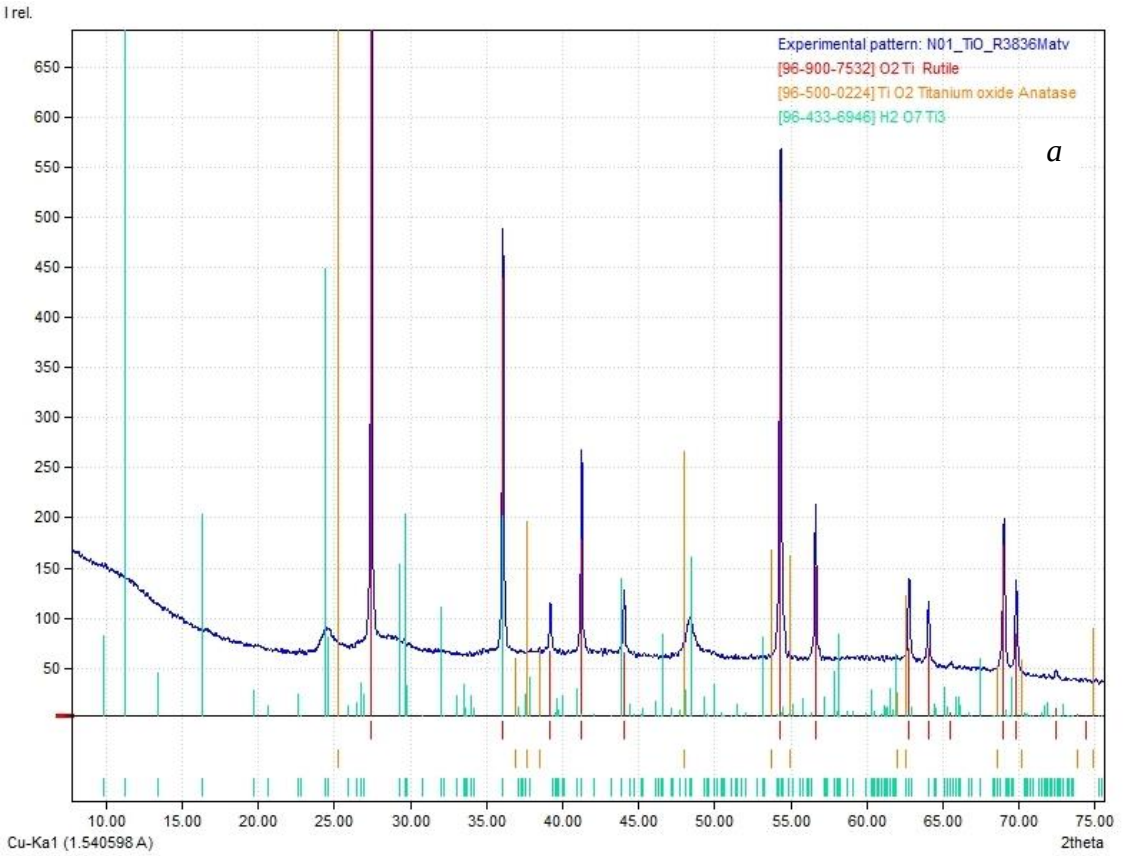
I rel.
Experimental pattern: N01_TiO_R3836Matv
[96-900-7532] O2 Ti Rutile
[96-500-0224] Ti O2 Titanium oxide Anatase
[96-433-6946] H2 O7 Ti3
a
Cu-Ka1 (1.540598 A)
2theta

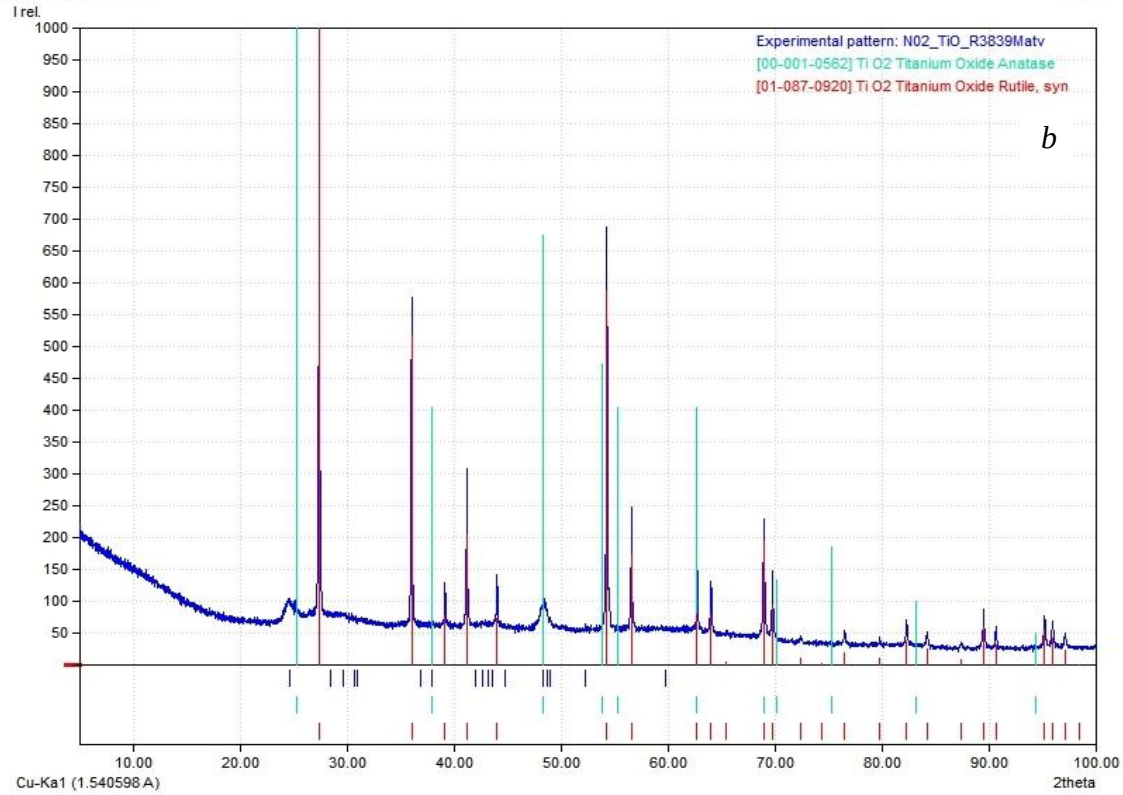
I rel.
Experimental pattern: N02_TiO_R3839Matv
[00-001-0562] Ti O2 Titanium Oxide Anatase
[01-087-0920] Ti O2 Titanium Oxide Rutile, syn
b
Cu-Ka1 (1.540598 A)
2theta

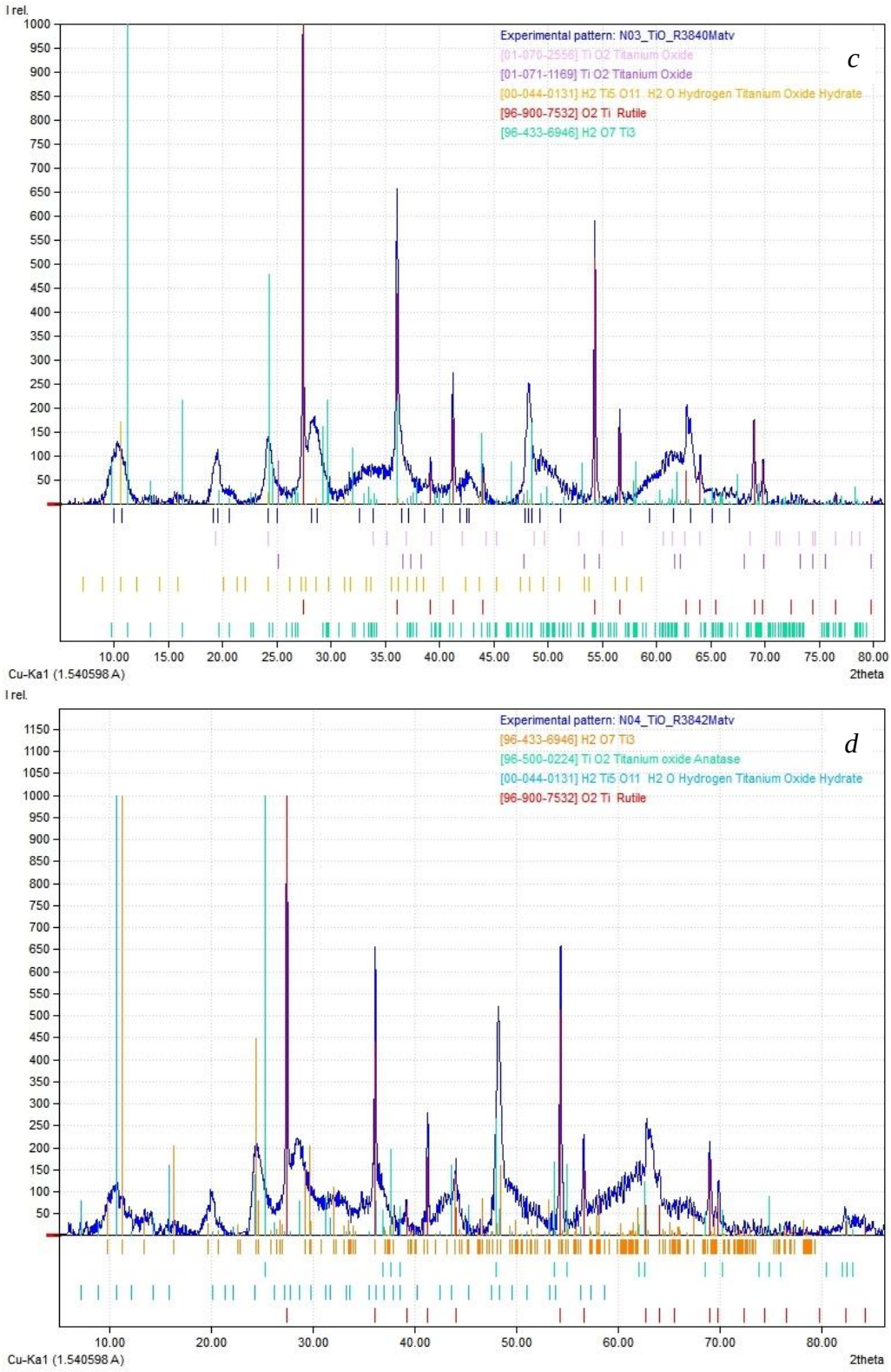

Fig. 4. XRD spectrum of TiO_2 nanotube samples synthesized via the ultrasonic–hydrothermal method
a – *d* – 4; 6; 8; 10 h
Рис. 4. Графики РСА анализа образцов нанотрубок TiO_2:
a – *d* – 4; 6; 8; 10 ч

The dissolution process liberates $Ti(OH)_6^{2-}$ species, which subsequently condense and reorganize into layered sodium titanates, leading to the steady increase of titanate content and concurrent reduction of rutile and anatase fractions. Prolonged hydrothermal treat ment, therefore, promotes the thermodynamically favored growth of titanate structures over the retention of rutile crystallites.

Simulated Rietveld-Based Phase Composition Analysis (Semi-Quantitative Estimation)
Смоделированный фазовый состав на основе анализа Ритвельда (полуколичественная оценка)

Hydrothermal Treatment Time, hours	Rutile Content, % w/w	Anatase Content, % w/w	Titanate Content, % w/w	Key Observations
4	~75 – 80	~15	~5 – 10	Rutile phase dominates; sharp and intense diffraction peaks indicate high crystallinity
6	~60 – 65	~25	~10 – 15	Anatase phase becomes more evident; moderate presence of titanate
8	~35 – 40	~10	~50 – 55	Titanate phase significantly increases; rutile phase weakens
10	~20	~5	~75	Titanate phase is predominant; rutile phase is minimal

Ultrasonic assistance intensifies this process by inducing acoustic cavitation, which generates localized high-temperature and high-pressure microdomains, enhances mass transfer, and fragments primary crystallites, thereby increasing the surface area available for nucleation. These effects collectively lower the kinetic barrier of the rutile-to-titanate transformation and accelerate structural reorganization, explaining the predominance of titanate after extended treatment times.

The difference between the XRD analysis results and Raman spectra clarifies the multiphase nature and the uneven distribution of the structure in TiO_2 nanotube materials, which directly affects their ability to store and release corrosion inhibitors. XRD primarily provides information about crystalline phases with high crystallinity and long-range order. At the same time, Raman spectra allow for detecting vibrational modes specific to local phases, with nanoscale size or those present at the surface-key factors in the adsorption and controlled release mechanisms of corrosion inhibitor molecules [26; 27]. The presence of the anatase phase, distinctly characterized by Raman spectra, is associated with a porous structure and a large surface area, which is favorable for storing inhibitors within the nanotube cavities. In contrast, phases such as rutile, identified in XRD analysis, have a dense structure with fewer defects, typically supporting a stable and controlled release process [20; 21]. Therefore, the difference between the XRD and Raman results is not contradictory but complementary, providing a comprehensive understanding of the phase transition process and structural distribution.

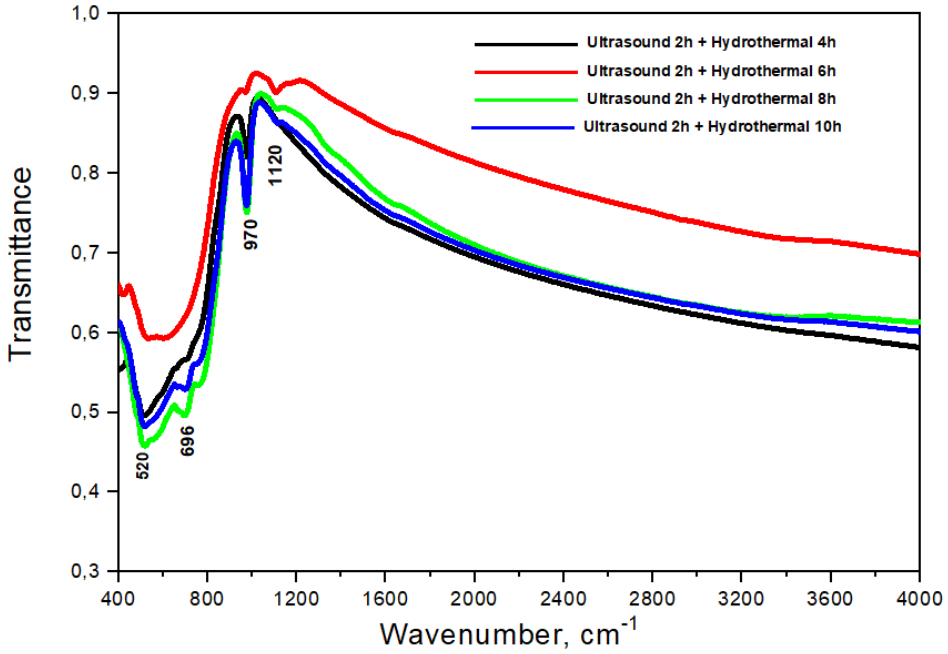

Fig. 5. FTIR spectra of nanotube samples synthesized by the combined ultrasonic-hydrothermal treatment method
Рис. 5. ИК-Фурье спектры образцов нанотрубок, синтезированных методом комбинированной ультразвуково-гидротермальной обработкой

The simultaneous combination of SEM, Raman spectroscopy, FTIR, and XRD methods enables a comprehensive observation, from external morphology to internal structure, thus clarifying the impact of synthesis conditions on corrosion inhibitors' storage and release capability. This approach also highlights the advantages of the hydrothermal method combined with ultrasonic treatment in creating controllable structure and function nanomaterials.

Conclusion

This evaluation study clarified the impact of reaction time, ranging from 4 to 10 hours, on the morphological characteristics, crystal structure, and corrosion inhibitor storage-release capacity of TiO_2 nanotube materials synthesized via the hydrothermal method combined with ultrasonic treatment. SEM analysis results show a significant change in the tube morphology, from a densely aggregated state to a more uniform distribution as the reaction time increases. At the same time, the Raman spectra and FTIR reflect a phase transition from anatase to rutile, with a gradual decrease in the presence of anatase-specific modes and an increase in rutile-specific vibrations. XRD analysis confirms the trend of increased crystallinity and changes in phase distribution over time, indicating the presence of intermediate phases such as titanates under certain conditions. The difference between Raman and XRD results is not contradictory but reflects the sensitivity of each method to different structural aspects, from surface vibrations to long-range crystal lattice order. The hydrothermal-ultrasonic method not only reduces the reaction time but also provides better control over the TiO_2 nanotube formation process, optimizing the structural properties for future improved anti-corrosion applications.

СПИСОК ЛИТЕРАТУРЫ

1. Kasuga T., Hiramatsu M., Hoson A., Sekino T., Niihara K. Формирование нанотрубки оксида титана. *Langmuir*. 1998;14(12):3160–3163. *https://doi.org/10.1021/la9713816*
2. Cui L., Hui K.N., Hui K.S. et al. Facile microwave-assisted hydrothermal synthesis of TiO_2 nanotubes. *Mater Lett*. 2012;75:175–178. *https://doi.org/10.1016/j.matlet.2012.02.004*
3. Dimas B.V., Hernández Pérez I., Febles V.G. et al. Atomic-scale investigation on the evolution of TiO_2-anatase prepared by a sonochemical route and treated with NaOH. *Materials*. 2020;13(3):685. *https://doi.org/10.3390/ma13030685*
4. Alkanad K., Hezam A., Al-Zaqri N. et al. One-step hydrothermal synthesis of anatase TiO_2 nanotubes for efficient photocatalytic CO_2 reduction. *ACS Omega*. 2022;7(43):38686–38699. *https://doi.org/10.1021/acsomega.2c04211*
5. Ou H.H., Lo S.L. Review of titania nanotubes synthesized via the hydrothermal treatment: Fabrication, modification, and application. *Sep Purif Technol*. 2007;58(1):179–191. *https://doi.org/10.1016/j.seppur.2007.07.017*
6. Zavala M.Á.L., Morales S.A.L., Ávila-Santos M.S. Synthesis of stable TiO_2 nanotubes: effect of hydrothermal treatment, acid washing and annealing temperature. *Heliyon*. 2017;3(11):e00456. *https://doi.org/10.1016/j.heliyon.2017.e00456*
7. Shi Y., Li R., Lei Z. Influences of synthetic parameters on morphology and growth of high entropy oxide nanotube arrays. *Coatings*. 2022;13(1):46. *https://doi.org/10.3390/coatings13010046*
8. Parinov I.A., Chang S.H., Gupta V.K., editors. Advanced Materials: Proceedings of the International Conference on “Physics and Mechanics of New Materials and Their Applications.” Springer International Publishing; 2018.
9. Liu N., Chen X., Zhang J., Schwank J.W. A review on TiO_2-based nanotubes synthesized via hydrothermal method: Formation mechanism, structure modification, and photocatalytic applications. *Catal Today*. 2014;225:34–51. *https://doi.org/10.1016/j.cattod.2013.10.090*
10. Niu L., Zhao X., Tang Z. et al. Difference in performance and mechanism for methylene blue when TiO_2 nanoparticles are converted to nanotubes. *J. Clean Prod*. 2021;297:126498. *https://doi.org/10.1016/j.jclepro.2021.126498*
11. Muresan L.M. Nanocomposite coatings for anti-corrosion properties of metallic substrates. *Materials*. 2023;16(14):5092. *https://doi.org/10.3390/ma16145092*
12. Kumar N., Sharma A. Surface coatings and functionalization strategies for corrosion mitigation. *American Chemical Society*. 2022;291–316. *https://doi.org/10.1021/bk-2022-1418.ch014*
13. Kumar S.S., Kakooei S. Container-based smart nanocoatings for corrosion protection. In: *Corrosion Protection at the Nanoscale*. 2020;403–421. *https://doi.org/10.1016/B978-0-12-819359-4.00021-0*
14. Ubaid F., Naeem N., Shakoor R.A., Kahraman R., Mansour S., Zekri A. Effect of concentration of DOC loaded TiO_2 nanotubes on the corrosion behavior of smart coatings. *Ceram Int*. 2019;45(8):10492–10500. *https://doi.org/10.1016/j.ceramint.2019.02.111*
15. Ву В.З., Нигметзянов Р.И. Обзор защиты от коррозии с помощью нанонитей TiO_2 и нанотрубок БТА/TiO_2, диспергированных в эпоксидной смоле, и предлагаемый метод

получения антикоррозионного покрытия из этого материала с помощью ультразвука. *Chem Bull*. 2025;8(1):2. *https://doi.org/10.58224/2619-0575-2025-8-1-2*

16. Rajamahendran T., Kasinathan K., Sivakumar R. et al. Effects of hydrothermal temperature and time on the structural and morphology of TiO_2 nanotubes and functionalization with sulfonic acid. *AIP Conf Proc*. 2021;2401(1). *https://doi.org/10.1063/5.0072985*

17. Chen H., Chen D., Bai L., Shu K. Hydrothermal synthesis and electrochemical properties of TiO_2 nanotubes as an anode material for lithium ion batteries. *Int J Electrochem Sci*. 2018;13(2):2118–2125. *https://doi.org/10.20964/2018.02.75*

18. Ohsaka T., Izumi F., Fujiki Y. Raman spectrum of anatase, TiO_2. *J. Raman Spectrosc*. 1978;7(6):321–324. *https://doi.org/10.1002/jrs.1250070606*

19. Frank O., Zukalova M., Laskova B. et al. Raman spectra of titanium dioxide (anatase, rutile) with identified oxygen isotopes (16, 17, 18). *Phys Chem Chem Phys*. 2012;14(42):14567–14572. *https://doi.org/10.1039/C2CP42763J*

20. Ubaid F., Naeem N., Shakoor R.A. et al. Effect of concentration of DOC loaded TiO_2 nanotubes on the corrosion behavior of smart coatings. *Ceram Int*. 2019;45(8):10492–10500. *https://doi.org/10.1016/j.ceramint.2019.02.111*

21. Chen H., Chen D., Bai L., Shu K. Hydrothermal synthesis and electrochemical properties of TiO_2 nanotubes as an anode material for lithium ion batteries. *Int J Electrochem Sci*. 2018;13(2):2118–2125. *https://doi.org/10.20964/2018.02.75*

22. Lacks D.J., Gordon R.G. Crystal-structure calculations with distorted ions. *Phys Rev B*. 1993;48(5):2889. *https://doi.org/10.1103/PhysRevB.48.2889*

23. Swamy V., Dubrovinsky L.S., Dubrovinskaia N.A. et al. Size effects on the structure and phase transition behavior of baddeleyite TiO_2. *Solid State Commun*. 2005;134(8):541–546. *https://doi.org/10.1016/j.ssc.2005.02.035*

24. Dimitrijevic N.M., Saponjic Z.V., Rabatic B.M., Poluektov O.G., Rajh T. Effect of size and shape of nanocrystalline TiO_2 on photogenerated charges: an EPR study. *J. Phys Chem C*. 2007;111(40):14597–14601. *https://doi.org/10.1021/jp0756395*

25. Niu L., Zhao X., Tang Z., Lv H., Wu F., Wang X. et al. Difference in performance and mechanism for methylene blue when TiO_2 nanoparticles are converted to nanotubes. *J. Clean Prod*. 2021;297:126498. *https://doi.org/10.1016/j.jclepro.2021.126498*

26. Bunaciu A.A., Udriştioiu E.G., Aboul-Enein H.Y. X-ray diffraction: instrumentation and applications. *Crit Rev Anal Chem*. 2015;45(4):289–299. *https://doi.org/10.1080/10408347.2014.949616*

27. Jin S., Smith E.M. Raman Spectroscopy and X-Ray Diffraction: Phase Identification of Gem Minerals and Other Species. Gems Gemol. 2024;60(4):518–535. *https://doi.org/10.5741/GEMS.60.4.518*

REFERENCES

1. Kasuga T., Hiramatsu M., Hoson A., Sekino T., Niihara K. Formation of titanium oxide nanotubes. *Langmuir*. 1998;14(12):3160–3163. *https://doi.org/10.1021/la9713816*

2. Cui L., Hui K.N., Hui K.S. et al. Facile microwave-assisted hydrothermal synthesis of TiO_2 nanotubes. *Mater Lett*. 2012;75:175–178. *https://doi.org/10.1016/j.matlet.2012.02.004*

3. Dimas B.V., Hernández Pérez I., Febles V.G. et al. Atomic-scale investigation on the evolution of TiO_2-anatase prepared by a sonochemical route and treated with NaOH. *Materials*. 2020;13(3):685. *https://doi.org/10.3390/ma13030685*

4. Alkanad K., Hezam A., Al-Zaqri N. et al. One-step hydrothermal synthesis of anatase TiO_2 nanotubes for efficient photocatalytic CO_2 reduction. *ACS Omega*. 2022;7(43):38686–38699. *https://doi.org/10.1021/acsomega.2c04211*

5. Ou H.H., Lo S.L. Review of titania nanotubes synthesized via the hydrothermal treatment: Fabrication, modification, and application. *Sep Purif Technol*. 2007;58(1):179–191. *https://doi.org/10.1016/j.seppur.2007.07.017*

6. Zavala M.Á.L., Morales S.A.L., Ávila-Santos M.S. Synthesis of stable TiO_2 nanotubes: effect of hydrothermal treatment, acid washing and annealing temperature. *Heliyon*. 2017;3(11):e00456. *https://doi.org/10.1016/j.heliyon.2017.e00456*

7. Shi Y., Li R., Lei Z. Influences of synthetic parameters on morphology and growth of high entropy oxide nanotube arrays. *Coatings*. 2022;13(1):46. *https://doi.org/10.3390/coatings13010046*

8. Parinov I.A., Chang S.H., Gupta V.K., editors. *Advanced Materials: Proceedings of the International Conference on "Physics and Mechanics of New Materials and Their Applications.*" Springer International Publishing; 2018.

9. Liu N., Chen X., Zhang J., Schwank J.W. A review on TiO_2-based nanotubes synthesized via hydrothermal method: Formation mechanism, structure modification, and photocatalyt-

ic applications. *Catal Today*. 2014;225:34–51. *https://doi.org/10.1016/j.cattod.2013.10.090*

10. Niu L., Zhao X., Tang Z. et al. Difference in performance and mechanism for methylene blue when TiO_2 nanoparticles are converted to nanotubes. *J. Clean Prod*. 2021;297:126498. *https://doi.org/10.1016/j.jclepro.2021.126498*

11. Muresan L.M. Nanocomposite coatings for anti-corrosion properties of metallic substrates. *Materials*. 2023;16(14):5092. *https://doi.org/10.3390/ma16145092*

12. Kumar N., Sharma A. Surface coatings and functionalization strategies for corrosion mitigation. *American Chemical Society*. 2022;291–316. *https://doi.org/10.1021/bk-2022-1418.ch014*

13. Kumar S.S., Kakooei S. Container-based smart nanocoatings for corrosion protection. In: *Corrosion Protection at the Nanoscale*. 2020;403–421. *https://doi.org/10.1016/B978-0-12-819359-4.00021-0*

14. Ubaid F., Naeem N., Shakoor R.A., Kahraman R., Mansour S., Zekri A. Effect of concentration of DOC loaded TiO_2 nanotubes on the corrosion behavior of smart coatings. *Ceram Int*. 2019;45(8):10492–10500. *https://doi.org/10.1016/j.ceramint.2019.02.111*

15. Wu V.Z., Nigmetzyanov R.I. The Review of corrosion protection by nanotubes TiO_2 and BTA/TiO_2 nanotubes dispersed in Epoxy and proposed method for preparation of anti-corrosion coating from this material assisted by ultrasound. *Chem Bull*. 2025;8(1):2. *https://doi.org/10.58224/2619-0575-2025-8-1-2*

16. Rajamahendran T., Kasinathan K., Sivakumar R. et al. Effects of hydrothermal temperature and time on the structural and morphology of TiO_2 nanotubes and functionalization with sulfonic acid. *AIP Conf Proc*. 2021;2401(1). *https://doi.org/10.1063/5.0072985*

17. Chen H., Chen D., Bai L., Shu K. Hydrothermal synthesis and electrochemical properties of TiO_2 nanotubes as an anode material for lithium ion batteries. *Int J Electrochem Sci*. 2018;13(2):2118–2125. *https://doi.org/10.20964/2018.02.75*

18. Ohsaka T., Izumi F., Fujiki Y. Raman spectrum of anatase, TiO_2. *J. Raman Spectrosc*. 1978;7(6):321–324. *https://doi.org/10.1002/jrs.1250070606*

19. Frank O., Zukalova M., Laskova B. et al. Raman spectra of titanium dioxide (anatase, rutile) with identified oxygen isotopes (16, 17, 18). *Phys Chem Chem Phys*. 2012;14(42):14567–14572. *https://doi.org/10.1039/C2CP42763J*

20. Ubaid F., Naeem N., Shakoor R.A. et al. Effect of concentration of DOC loaded TiO_2 nanotubes on the corrosion behavior of smart coatings. *Ceram Int.* 2019;45(8):10492–10500. *https://doi.org/10.1016/j.ceramint.2019.02.111*

21. Rao B.M., Roy S.C. Anatase TiO_2 nanotube arrays with high temperature stability. RSC Adv. 2014;4(72):38133–38139. https://doi.org/10.1039/C4RA05882H

22. Lacks D.J., Gordon R.G. Crystal-structure calculations with distorted ions. *Phys Rev B.* 1993;48(5):2889. *https://doi.org/10.1103/PhysRevB.48.2889*

23. Swamy V., Dubrovinsky L.S., Dubrovinskaia N.A. et al. Size effects on the structure and phase transition behavior of baddeleyite TiO_2. *Solid State Commun*. 2005;134(8):541–546. *https://doi.org/10.1016/j.ssc.2005.02.035*

24. Dimitrijevic N.M., Saponjic Z.V., Rabatic B.M., Poluektov O.G., Rajh T. Effect of size and shape of nanocrystalline TiO_2 on photogenerated charges: an EPR study. *J. Phys Chem C.* 2007;111(40):14597–14601. *https://doi.org/10.1021/jp0756395*

25. Niu L., Zhao X., Tang Z., Lv H., Wu F., Wang X. et al. Difference in performance and mechanism for methylene blue when TiO_2 nanoparticles are converted to nanotubes. *J. Clean Prod*. 2021;297:126498. *https://doi.org/10.1016/j.jclepro.2021.126498*

26. Bunaciu A.A., Udriştioiu E.G., Aboul-Enein H.Y. X-ray diffraction: instrumentation and applications. *Crit Rev Anal Chem.* 2015;45(4):289–299. *https://doi.org/10.1080/10408347.2014.949616*

27. Jin S., Smith E.M. Raman Spectroscopy and X-Ray Diffraction: Phase Identification of Gem Minerals and Other Species. Gems Gemol. 2024;60(4):518–535. *https://doi.org/10.5741/GEMS.60.4.518*

Information about the authors

Van Zung Vu, *PhD student, Department of Structural Materials Technology, specialization,* Moscow Automobile and Road Construction State Technical University
E-mail: vandunph2605@gmail.com
ORCID: 0009-0000-0660-0144

***Huy Bach* Nguyen**, *Student, Faculty of Energy and Environmental Engineering,* Moscow Automobile and Road Construction State Technical University
E-mail: huybach484@gmail.com
ORCID: 0009-0008-4597-7567

Ravil I. Nigmetzyanov, *Cand. Sci. (Eng.), Associate Professor, Department of Structural Materials Technology,* Moscow Automobile and Road Construction State Technical University
E-mail: lefmo@yandex.ru
ORCID: 0009-0008-1443-7584

Сведения об авторах:
Ван Зунг Ву, *аспирант кафедры «Технология конструкционных материалов»,* Московский автомобильно-дорожный государственный технический университет
E-mail: vandunph2605@gmail.com
ORCID: 0009-0000-0660-0144

Хю Бач Нгуен, *студент факультета «Энергоэкологический»,* Московский автомобильно-дорожный государственный технический университет
E-mail: huybach484@gmail.com
ORCID: 0009-0008-4597-7567

Равиль Исламович Нигметзянов, *к.т.н., доцент кафедры «Технология конструкционных материалов»,* Московский автомобильно-дорожный государственный технический университет
E-mail: lefmo@yandex.ru
ORCID: 0009-0008-1443-7584

Авторы заявляют об отсутствии конфликта интересов.
The authors declare that there is no conflict of interest.

Поступила в редакцию 24.06.2025
После доработки 30.07.2025
Принята к публикации 04.08.2025

Received24.06.2025
Revised 30.07.2025
Accepted 04.08.2025